Journal of Medicinal Chemistry

Article

pubs.acs.org/jmc

Diastereotopic and Deuterium Effects in Gemini

Hubert Maehr,*[,†] Natacha Rochel,[‡] Hong Jin Lee,[†,∥] Nanjoo Suh,[†,§] and Milan R. Uskokovic[†]

[†]Department of Chemical Biology, Ernest Mario School of Pharmacy, Rutgers, The State University of New Jersey, 164 Frelinghuysen Road, Piscataway, New Jersey 08854, United States

[‡]Département de Biologie et de Génomique Structurales, Institut de Génétique et de Biologie Moléculaire et Cellulaire (IGBMC), Centre National de la Recherche Scientifique, Institut National de la Santé de la Recherche Médicale, Université de Strasbourg, 1 rue Laurent Fries, 67404 Illkirch, France

[§]The Cancer Institute of New Jersey, 195 Little Albany Street, New Brunswick, New Jersey 08903, United States

S *Supporting Information*

ABSTRACT: Changing the geminal methyl groups on 1α,25-dihydroxyvitamin D_3 and its analogues to the deuterio versions generally improves the bioactivity. Derivatives of 1α,25-dihydroxyvitamin D_3 with two chains emanating at C20, commonly referred to as gemini, are subject to the same phenomenon. Additionally, gemini with different side chains are susceptible to bioactivity differentials where the C17−C20 threo configuration usually imparts higher activity than the corresponding erythro arrangement. In an effort to analyze the deuterium effect on gemini with minimal diastereotopic distortion, we synthesized gemini with equal side chains but introduced deuterium diastereospecifically on either chain. We solved the crystal structures of these compounds in the zebra fish zVDR ligand binding domain as complexes with NCoA-2 coactivator peptide and correlated the findings with growth inhibition in a breast cancer cell line.

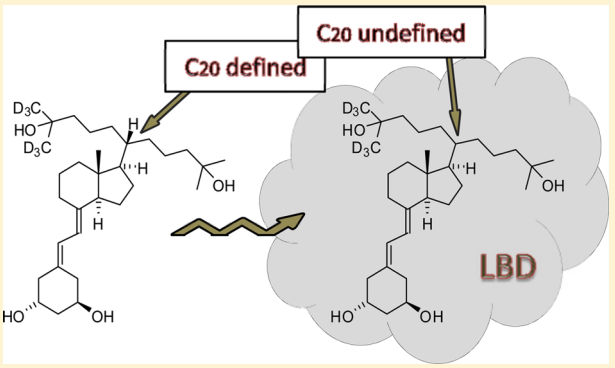

INTRODUCTION

Modification of the chemical structure of drugs to prevent or retard metabolic degradation is an important activity in drug optimization and requires an alteration of the sites of metabolic activity so that it is no longer a suitable substrate for the enzyme that initiates the metabolism. Addition of substituents and protective groups and changes to groups of different size and polarity are commonly employed for this purpose.[1] Although isotopology is an extremely useful tool in metabolism studies, its application as a modifier of drug metabolism is restricted to deuterium[2,3] which has the renown of rendering the intrinsic drug properties invariant.

In the vitamin D arena, molecular transmutations of 1α,25-dihydroxyvitamin D_3 (**1**, 1α,25-$(OH)_2D_3$, or calcitriol) have been pursued not only with the aim of metabolic stabilization but also to modify the biological properties that reach beyond calcium and phosphorus metabolism and act as agonists in transcriptional activities involving carcinogenesis, immune disorders, and skin diseases. Tailored modifications, intended to reach specifically but one of those goals, have proved to be nontrivial as small chemical changes in the ligand enable conformational changes in the VDR ligand-binding domain (LBD) with notoriously far-reaching consequences by affecting the central role of the hormone in calcium and bone metabolism and the molecular switch mechanism of nuclear 1α,25-$(OH)_2D_3$ signaling. This molecular switch comprises the complex of the vitamin D receptor (VDR), the retinoid X receptor (RXR), and a 1α,25-$(OH)_2D_3$ response element (VDRE). It functions through the LBD of the VDR that is ligand-stabilized in either agonistic, antagonistic, or non-agonistic conformation,[4] all depending on ligand constitution and configuration. Similarly, DRIP (vitamin D receptor interacting protein) mediated interactions have been invoked as ligand-dependent phenomena and potentially creating aberrant biological responses.[5,6] Extending C21 of 1α,25-$(OH)_2D_3$ and its derivatives to a second side chain as in **3**, **4**, and **5** gave rise to a new class of derivatives, known as gemini, that significantly augment the biological spectrum of 1α,25-$(OH)_2D_3$ on various fronts.[7−12] These compounds double the opportunity for chain modifications and offer exploitation of newly generated stereochemical consequences.

With a focus on metabolic stability, we studied, some 30 years ago, the stimulation of cartilage growth in vitro by **1** in two growing-cartilage models, the avian pelvic cartilage, and the mammalian scapular growth-plate cartilage, known to be susceptive to vitamin D regulation.[13] In that study, we discovered that **1**, whose geminal methyl groups in the side chain were replaced with deuteriomethyl moieties, exhibited superior activity in the growth-plate cartilage model. This

Received: January 7, 2013

dx.doi.org/10.1021/jm400032t | *J. Med. Chem.* XXXX, XXX, XXX−XXX

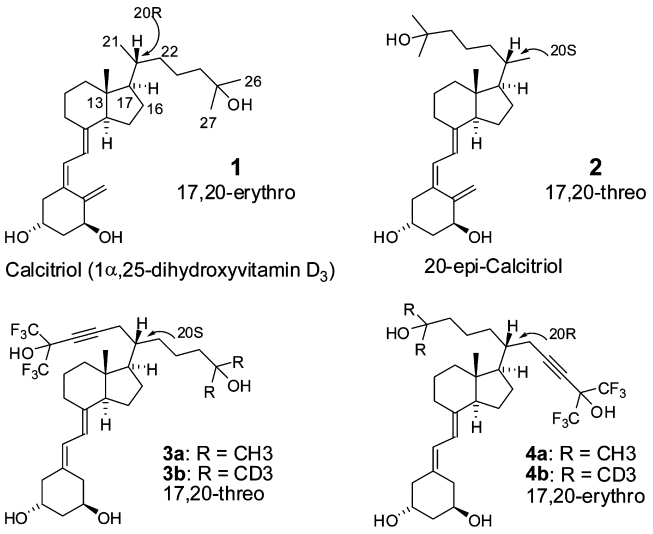

"deuterium effect" in biological systems has since been verified by us in a number of 1α,25-$(OH)_2D_3$ derivatives and is now being exploited by commercial enterprises that dwell specifically on the deuteration of existing drugs in search of novelty and modified biological properties and activities.[14]

Subsequent to our original observation, we also synthesized a number of 1α,25-$(OH)_2D_3$ derivatives in the gemini series, wherein geminal methyl groups were transmuted to perdeuterio equivalents.[15−17] In all instances, these derivatives were biologically more active than the protio parents. The reason for this elevation of activity is not entirely clear. Because side chain degradation of 1α,25-$(OH)_2D_3$ is recognized as the initial step toward drug inactivation and excretion, and positions 23, 24, and 26 are known sites of oxidative degradation, one could indeed infer, a priori, magnified activity of the deuterio versions as the direct result of increased metabolic stability. The metabolic events, however, point to calcitroic acid as the major excretory form of the hormone, which is produced by the inducible, mitochondrial cytochrome P450 (CYP24) by initial C24 hydroxylation and oxidation, followed by hydroxylation at C23 and cleavage of the C23−C24 bond.[18,19] This mechanism also appears to hold for gemini and its derivatives, as it has been shown that gemini suffers diasterospecific C24 hydroxylation as the first step in the metabolic process.[20] Although the deuterium−carbon bond is some 10 times stronger than the hydrogen−carbon bond, the argument of bond strength in support of metabolic stability enhancement as primary isotope effect is untenable because the deuterio modification occurs at the geminal methyl groups and cleavage of a C−D bond at either C26 or C27 cannot be implicated in the rate-determining step in the major metabolic pathway. Formation and further metabolism of a lactone, corresponding to 1α,25-dihydroxyvitamin D_3-26,23-lactone[21] and initiated by C23 and C26 oxidations, is also an unsatisfactory explanation of the deuterium effect because the expected oxidation intermediates[22] remain undetected.[20] A similar argument can be made against other minor pathways[23] including a conceivable metabolism via initial C20- and C22-hydroxylations.[24]

In the absence of metabolic involvement, the site of isotopic changes exclusively at the geminal methyl groups at the crowded termini should, per expectations, only infinitesimally affect the physicochemical properties and be insufficient to induce conformational changes in the LBD. In this account, we intend to illuminate the "biological deuterium effect" in gemini, which is not only a function of deuterioisotopology alone but further obfuscated by diastereotopicity in molecules with two unequal chains.

To shed some light onto these stereochemical and deuterium effects of 1α,25-$(OH)_2D_3$ and its congeners, it is appropriate to review briefly the observed biological consequences resulting from diastereotopic and isotopological changes. The examples that permit such comparisons are few but are indicative of certain trends. Current emphasis is placed exclusively on the chirality at C20 and the effect of deuteriomethyl groups at the chain termini corresponding to C26 and C27 in **1**.

Commencing with the C20 chirality issue, it is known that epi-1α,25-$(OH)_2D_3$ (**2**) shows exceptionally high affinity to the vitamin D receptor due to altered protein binding;[25] it is a more potent inducer of cell differentiation than **1**, it is transcriptionally more active by some 3 powers of magnitude, it is metabolized 36 times slower than **1**, it showed decreased DBP (rat plasma) binding affinity but is bound to the bovine thymus VDR with 5 times greater affinity than **1**,[26] it is a more powerful regulator of cell cycle progression, and it was concluded that **2** protected the VDR against catabolism more efficiently than **1** by preventing, or retarding, the binding of factors mediating VDR degradation.[27] In a comparison of **1** and **2**, one can now aver that **2** is more active due to its 20S configuration. The recognition of stereochemical details in crystallographic images is facilitated by viewing the stereocenter C20 as a unit with the contiguous and configurationally defined C17. Thus rephrasing, the compound where the C17−C20 bond is of the threo configuration is more active.

It has been shown that 1α,25-$(OH)_2D_3$ and its derivatives assume very similar positions of their A-seco-B, C, and D-rings in the VDR LBD where locus and configuration are enforced by well-defined sets of interactions.[28−31] The ease of side chain accommodation of either **1** or **2** in the same channel apparently renders irrelevant the rotational barrier that the required change of the torsion angle at C17−C20 entails. Figure1 shows

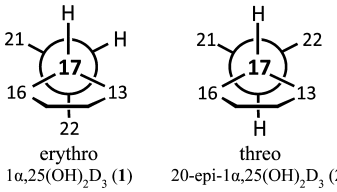

Figure 1.

simulated views of **1** and **2** from the proximal C17 to the distal C20 with synclinal and antiperiplanar dihedral angles of the hydrogen atoms, respectively, suggesting lower ground state energy of the threo configuration. These simplified representation convey the similarity with the corresponding arrangements discernible in the crystal structures of VDR LBD complexes of compounds derived from either **1** or **2**.[32] Although the same channel is occupied by **1** or **2**, the chains line opposite sides in the pocket and consequently engage in different protein interactions.

Following the discovery that the parental gemini **5** exhibited enhanced antiproliferative activities compared to **1**,[7] it was found that the structures of zVDR-**5** and zVDR-**1** were similar but the accommodation of the second side chain in **5** induced a backbone shift and side chain reorientation. This ligand-dictated structural rearrangement of the protein core preserved the original space used by the 1α,25-$(OH)_2D_3$ chain in **1** and **2**

dx.doi.org/10.1021/jm400032t | J. Med. Chem. XXXX, XXX, XXX−XXX

(referred to as the parental channel). This core is also able to accommodate one of the gemini chains, but in addition, the change of the protein core made possible the creation of a new pocket (referred to as the "secondary channel") to accept the second chain.[32]

Given the choice between the aliphatic or alkyne chains present in **3** and **4**, it was shown that it is the larger alkyne side chain that prefers the parental channel. The smaller and more flexible aliphatic chain pushed for accommodation by creating the new pocket resulting in superagonist activity due to increased stabilization of helix H12.[31,33] Considering that **2** is more potent in a biological sense than **1**, and considering only the size of the side chains, one can surmise that the threo pair **3a**/**3b** should elicit higher bioactivity than the erythro pair **4a**/**4b**. The gemini pairs **3a**/**4a** and **3b**/**4b** are thus examined with respect to C20 epimerism and the pairs **3a**/**3b** and **4a**/**4b** with respect to the deuterium effect.

Probing first into this "threo effect," we observed varying degrees of differences in biological responses among the available compounds. The threo compound **3a** was three times more calcemic than either of the erythro compounds **1** or **4a** but some 500 times more potent in interferon-γ release. In a tumor-growth model in mice, both **1** and **4a** showed no significant effect at 0.02 μg, whereas **3a** exhibited a dose-dependent response with tumor volume reduction of 41% at the same dose. In a study of estrogen receptor (ER)-positive carcinomas in rats, however, **3b** and **4b** were equally active in the inhibition of NMU-induced breast cancer carcinogenesis in disregard of the threo effect.[15,17]

Investigating the deuterium effect, we found **3a** and **3b** in the tumor-growth model in mice with dose-dependent differences, but the deuterio compound **3b** was 10 times as active as the protio version **3a**. These observations raised new questions. In the absence of a diastereotopic bias, would a change to the geminal trideuteriomethyl groups in gemini alone suffice to change the biological properties of the ligand; i.e., would there be a difference between the parental gemini **5** and its dodecadeuterio version **6**? And if it does, could the ligand properties be further refined through the reintroduction of a diastereochemical bias in **6** by replacing just one set of the geminal deuteriomethyl groups with the corresponding protio versions? If the deuterium effect would still be observed, would it then matter which of the side chains carries the deuteriomethyl groups? In other words, would the threo-effect still be palpable in molecules whose chemical constitutions differ so little from each other?

RESULTS AND DISCUSSION

To provide the tools for the answers to these intriguing questions, we synthesized dodecadeuteriogemini **6**, the "threo" hexadeuteriogemini **7a**, and the 19-nor analogue **7b**, as well as the corresponding erythro pair **8a** and **8b** as described hereunder. The synthetic concept used for the generation of **6** differs from the published methods employed for the protio analogue **5b**.[34,35] According to those procedures, both side chains were introduced concurrently; the construction of **7** and **8**, however, required a stepwise process. Thus, we chose **6** as a test candidate for the consecutive side chain assembly starting with **10**, which was then paradigmatic for the preparation of **7** and **8**. The synthetic steps are illustrated in Scheme 1.

The syntheses commenced with the previously prepared alkenes **10**[16] and **16**[36] derived from methyl ester **9**. Hydroboration of **10**, with oxidative workup, gave **11** as a

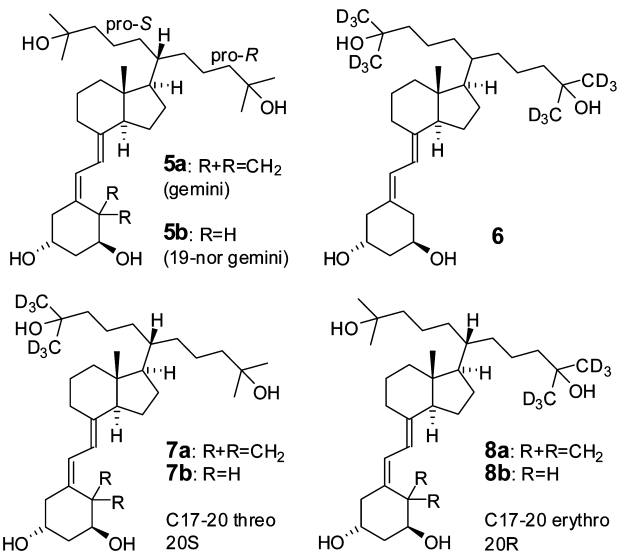

diastereomeric mixture, and a subsequent treatment with iodine/triphenylphosphorane/imidazole in DCM afforded the diastereomeric iodo compound **12** using protocols previously established for the preparation of **18** and **23**.[20] The second chain was constructed from **12** by the Sustmann addition process to ethyl acrylate.[37] The resulting diastereomeric mixture of ethyl esters **13** was treated with deuteriomethylmagnesium iodide in ether to afford the diol **14a** as a single stereoisomer. Cleavage of the *t*-butyldimethylsilyloxy group with fluorosilicic acid[38] gave the triol **14b**, which was oxidized with pyridinium dichromate in DCM to lead to the ketone **15a**. This ketone was converted to the bis-trimethylsilyl ether **15b** because it was found that it gave better yields in the subsequent coupling reaction than the diol **15a**. This additional operation is insignificant because the required deprotection proceeds concurrently with the compulsory desilylation of the two protective groups in the A-ring after the coupling reaction.

On the basis of the successful construction of the coupling partner **15b**, we prepared the diastereomeric ketones **21b** and **26b** analogously, as illustrated in Scheme 1. Commencing with the iodo-pairs **18** and **23** derived from the epimeric alcohols **17** and **22** as described previously, we repeated the chain extension leading to the esters **19** and **24**. Subsequent alkylations with deuteriomethylmagnesium iodide gave **20a** and **25a**, deprotections with fluorosilicic acid advanced the intermediates to the triols **20b** and **25b**, oxidations with pyridinium dichromate gave ketones **21a** and **26a**, and reprotections with trimethylsilyl imidazole furnished the coupling partners **21b** and **26b**.

The ketones **21b** and **26b** were coupled each with **30a**, prepared from carvone,[39,40] and **15b**, **21b**, and **26b** were coupled each with **30b**, prepared by total synthesis.[41] These coupling reactions were performed according to the established protocols propagated by Lythgoe[42] and illustrated in Scheme 2. The resulting tetrasilylethers **27** and the pairs **28a**/**28b** and **29a**/**29b** were desilylated with tetrabutylammonium fluoride in THF during disparate lengths of time to furnish the targets **6** and the pairs **7a**/**7b** and **8a**/**8b**, respectively.

With these compounds in hand, we investigated the orientations of the two epimeric compounds **7** and **8** within the LBD of the zVDR. If the LBD of the zVDR is given the choice between these C20 epimers, and if the zVDR is discriminating toward their chain constitutions, we should observe two distinct epimers in zVDR-**7** and zVDR-**8**

dx.doi.org/10.1021/jm400032t | J. Med. Chem. XXXX, XXX, XXX–XXX

Scheme 1

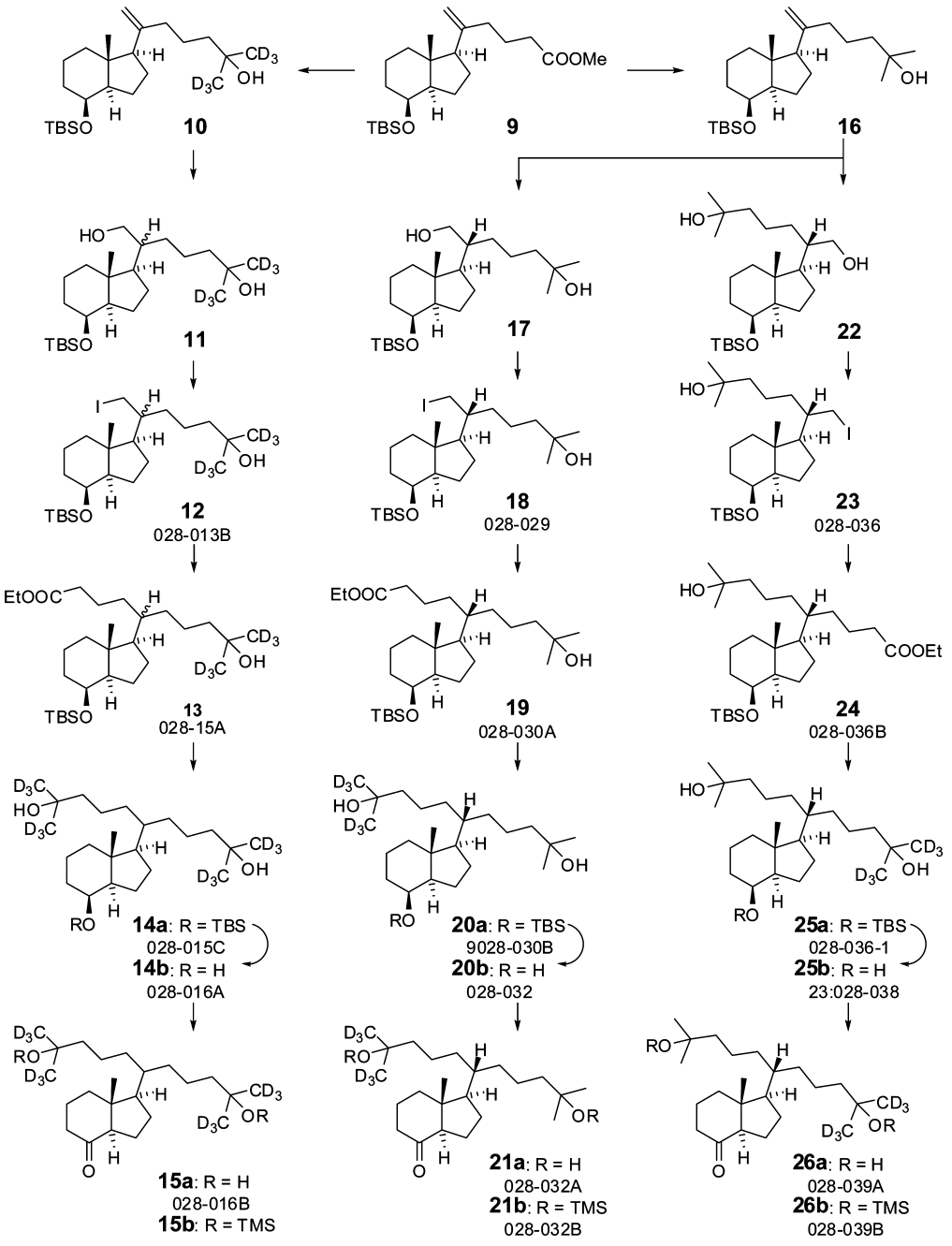

corresponding to the C17,20-threo and C17,20-erythro configurations depicted schematically in Figure 2, wherein C represents the side chain with geminal methyl groups as in **1** and D symbolizes the chain with deuteriomethyl groups corresponding to C21 in 1α,25-$(OH)_2D_3$. The "natural" chain of 1α,25-$(OH)_2D_3$ is allowed arbitrary occupancy in the parental channel. The view was changed from that in Figure 1, with C20 now as the proximal carbon, to facilitate a comparison with the crystal structure in Figure 3C discussed below. The illustration allows a perception of the conformational task which the side chains would have to undergo to secure accommodation in the same channel. Conversely, if the zVDR is promiscuous toward accommodating these side chain constitutions, the diastereotopicity of C20 with respect to the VDR vanishes and only one of the two configurations portrayed in Figure 2 would be discernible as the two chains are now indistinguishable.

We accomplished the crystal structure elucidations of the zebrafish zVDR LBD in complexes with **7a**, **7b**, **8a**, and **8b**, together with the NCoA-2 coactivator peptide. Similar to **5** or its derivatives **3a**/**b** and **4a**/**b**, the ligands **7a**, **7b**, **8a**, and **8b** induce, upon binding, the reorientation of the side chain of a Leu residue in helix 7 [Leu337] that allows the accommodation of the second side chain of such ligands (Figure 3A).[28,33] Both ligands make similar interactions with the protein and the hydroxyl groups of the analogues form similar hydrogen bonds as zVDR LBD bound to the parental gemini. For the 19-nor analogues, **7b** and **8b**, interactions with Leu261 (Helix3), Ser265 (Helix3), and Ile299 (Helix5) are lost compared to the natural A-ring compounds **7a** and **8a** (Figure 3B). These lost

dx.doi.org/10.1021/jm400032t | J. Med. Chem. XXXX, XXX, XXX–XXX

Scheme 2

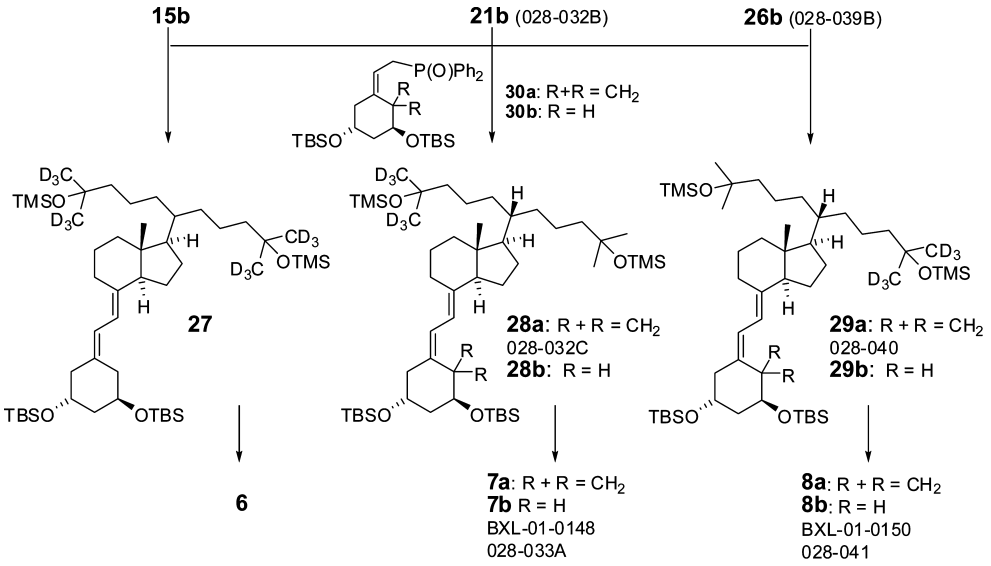

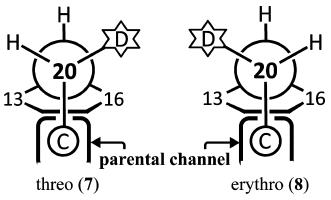

Figure 2.

interactions, notably with Ser265 that forms an anchoring H-bond interaction with the ligands, may explain their lower biological potency in the cell growth inhibition study presented below.

Looking now to the interactions of the side chains of the threo pair **7a**/**b** and the erythro pair **8a**/**8b** (Figure 3C), we find similar contacts with the protein for both pairs. The only observed difference within the threo pair **7a** and **7b** is a stronger interaction of C26 of **7a** with Ala331 at 3.7 Å compared to 4.0 Å for **7b**, again, in agreement with the difference in cell growth inhibition.

Because the configuration at C20, and hence the spacial arrangements of the protio- and deuterio-substituted side chains, are firmly defined by synthesis, it is inconsequential that the electron density maps of 7 and **8** do not allow a distinction between hydrogen and deuterium atoms. Most significantly, the medium resolutions of the crystal structures reveal no significant differences in the interactions, except for the one with Ala331 which is the result of the A-ring modification. An isotope-induced change in molecular conformation in one of the ligands, either the "erythro ligand" or the threo equivalent, to force the same specific side chain into the same specific channel of the LBD did not materialize, as evidenced by Figure 3C. Both ligands are nearly superimposable, i.e., only one conformation for both diastereotops is perceptible, which is diagrammatically shown in Figure 2 as the threo isomer with the positive dihedral angle between the hydrogen atoms. This arrangement is consistent with the crystal structure shown in Figure 3C.

As we have now shown that the zVDR does not distinguish between the closely related deuterio and protio side chains, compounds 7 and **8** maintain equal populations of the deuterio chains in either parental and secondary channel; i.e., the LBD is indifferent toward the diastereotopic relationship between 7 and **8**, rendering them not only equally active, but, thanks to the presence of one set of deuteriomethyl groups, distinctly more potent than **5**. Following this trend, one can predict that a compound with two sets of deuteriomethyl groups should be even more active than either **7b** and **8b** as both channels are

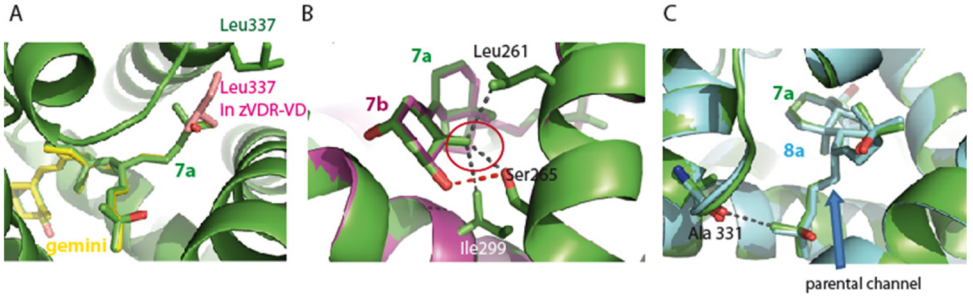

Figure 3. Crystal structures of zVDR LBD complexes. (A) Superposition of **7a** (green) with parental gemini (yellow) and 1α,25-$(OH)_2D_3$ (pink). Leu337 in zVDR complexes with gemini analogues adopts another conformation than in zVDR/1α,25-$(OH)_2D_3$ upon binding of the second side chain. (B) The 19-nor compound **7b** (pink) lost interactions with Leu261, Ser265, and Ile299 compared to the normal A-ring compound **7a** (green). Dark dashed lines indicate van der Waals interactions, and the red dashed line corresponds to hydrogen-bond interaction. (C) Superposition of **7a**, threo analogue (in green) with the erythro one **8a** (in cyan).

dx.doi.org/10.1021/jm400032t | J. Med. Chem. XXXX, XXX, XXX–XXX

occupied exclusively by deuterated chains. This prediction is upheld in the breast cancer MCF10CA1 growth inhibition study shown in Figure 4, where the dodcecadeuterio gemini **6**

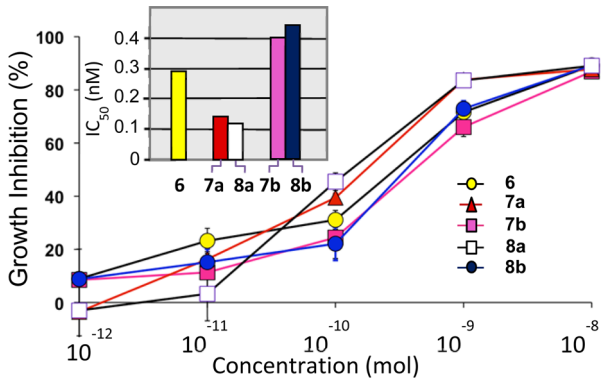

Figure 4.

appears to be more active than **7b** and **8b**, all of which containing the 19-nor A-ring. The activity differentials are highlighted by the IC_{50} values. Ligands **7b** and **8b** are nearly equipotent and so is the pair **7a**/**8a** which, in turn, is more potent by virtue of the natural A-ring as predicted by the binding anchors between Leu261, Ser265, and Ile299, which are absent in **7b**, as evident in Figure 3B.

CONCLUSIONS

The bioactivities of all vitamin D analogues tested so far benefit from a replacement of the geminal methyl groups with deuterio equivalents at the side chains. Gemini with significantly different side chains usually exhibit the "threo effect", i.e., the 20*S* epimers tend to be more active than the *R*-counterparts. This bias in biological activity appears to parallel the ability of the LBD to recognize C20 topographically. In the borderline scenario where the side chains differ only by deuteration, the topographic differential is minimal and no longer recognized by the LBD thus rendering the members of the pairs **7a**/**8a** and **7b**/**8b** equipotent.

Binding affinities between biomolecules can be subject to deuterium isotope effects on noncovalent interactions. More specifically, isotopic ligand modifications can affect van der Waals interactions with proteins and, in some cases, depending on the position of deuterium, stabilize or destabilize the binding of the ligand.[42] We are consonant with the hypothesis that the higher bioactivities of the "deuterio ligands" are the result of secondary kinetic deuterium effects eliciting a certain stabilization of the LBD of the VDR with enhanced coactivator interactions.

The findings presented herein provide additional guidelines for drug research, especially for future phenotypic drug discovery efforts in the area related to vitamin D.

EXPERIMENTAL SECTION

Crystallography. Purification and crystallization. The zebrafish VDR LBD (residues 156–453) was produced and purified as described.[29,33] The protein was concentrated using Amicon ultra-30 (Millipore) to 3–7 mg/mL and incubated with a 2-fold excess of ligand and a 3-fold excess of the coactivator NCoA-2 peptide (686-KHKILHRLLQDSS-698). Crystals were obtained in 50 mM Bis-Tris pH 6.5, 1.6 M lithium sulfate and 50 mM magnesium sulfate.

X-Ray Data Collection and Structure Determination. Protein crystals were mounted in a fiber loop and flash-cooled under a nitrogen flux after cryoprotection with oil (Hampton research). Data collection from a single frozen crystal was performed at 100 K at ESRF (Grenoble, France), beamline ID-14-1. The crystals are isomorphous and belong to the space group $P6_522$, with one LBD complex per asymmetric unit. The four structures were solved by molecular replacement and refined to 2.95, 2.44, 2.70, and 2.70 Å for zVDR/**7a**, zVDR/**7b**, zVDR/**8a**, and zVDR/**8b**, respectively. Diffraction data collection and structure refinement were obtained as described.[33]

Cell Growth Inhibition Studies. MCF10A1a human estrogen receptor (ER)-negative breast cancer cells were cultured in DMEM/F-12 medium with 5% heat-inactivated horse serum (Hyclone, Logan, UT) at 37 °C with 5% CO_2. The MCF10CA1a cells were passaged 2 times a week to maintain log phase growth. For testing growth inhibitory effects of gemini, MCF10CA1a cells were distributed in 24-well plates (5000 cells/well) and treated with gemini for 3 days. One μCi of [^{3}H] thymidine was added 3 h before the harvest. The cells were analyzed on a Beckman LS 6500 liquid scintillation counter.

Chemistry. Chemical reactions were monitored by TLC using silica gel 60 F_{254} plates (Merck), typically 5 cm high, and visualized with UV light or by treatment with phosphomolybdic acid (PMA). Solvents were of commercial sources but THF was freshly distilled from sodium benzophenone ketyl. The pH 7 phosphate buffer used occasionally during work up comprised 139.4 g of dipotassium phosphate in 400 mL of water plus 100 mL of 2 M phosphoric acid. Column chromatography was carried out on silica gel Merck 230–400 mesh ASTM, and fractions were pooled according to TLC profiles. Solutions were dried with sodium sulfate unless stated otherwise, and chemical operations were conducted under nitrogen or argon. Products were typically dried at ambient temperature at 1 Torr or below. Organolithium solutions were purchased from Aldrich and used at nominal molarities. Mass spectra were recorded on Waters ZQ (low resolution) and Bruker APEX II (high resolution) spectrometers. NMR spectra were obtained on a Varian INOVA 400 spectrometer at 25 C. The chemical shifts for ^{1}H spectra are referenced to $CHCl_3$ at 7.26 ppm and DMSO-d_5 at 2.50 ppm. For ^{13}C NMR spectra, the chemical shifts are referenced to $CDCl_3$ at 77.0 ppm and DMSO-d_6 at 39.5 ppm.

Ethyl 5-[(1*R*,3a*R*,4*S*,7a*R*)-4-[*tert*-Butyl(dimethyl)silyl]oxy-7a-methyl-1,2,3,3a,4,5,6,7-octahydroinden-1-yl]-10,10,10-trideuterio-9-hydroxy-9-(trideuteriomethyl)decanoate (13). To a vigorously stirred mixture comprising Zn powder (0.297 mg, 4.54 mmol), pyridine (5.6 mL), and ethyl acrylate (0.455 g, 4.54 mmol) was added nickel chloride hexahydrate (0.2682 g, 1.128 mmol). The gray suspension was warmed to 50 °C and after 10 min to 65 °C and stirred at that temperature for 30 min. During this time, the mixture quickly assumed a greenish and then a brown–red color. This mixture was then cooled in an ice bath, and a solution of **12** (0.517 g, 0.978 mmol) in pyridine (3.5 mL) was added. The ice bath was removed, and stirring continued at ambient temperature. Reaction progress was monitored by TLC (1:3 EtOAc–hexane), which showed the gradual conversion of **12** (R_f 0.70) to the ethyl ester **13**. The reaction was ca. 90% complete after 30 min, and after 3 h **12** was no longer detectable. The mixture was then poured into EtOAc (50 mL); the resulting suspension was filtered through Celite, the filter cake was washed with EtOAc (40 mL), filtrate and washings were equilibrated with 1 M HCl (2 × 50 mL) and 0.2 M phosphoric acid (40 mL) followed by brine (5 mL), an aqueous solution (25 mL) containing EDTA disodium salt dihydrate (0.60 g) and sodium hydrogen sulfate (0.60 g), and then with brine (5 mL). The solution was dried ($MgSO_4$) and evaporated. TLC of the residue showed two spots with very similar mobilities, commensurate with the diastereomeric nature of ester **13**. This material was further purified by flash chromatography, without intent to separate the mixture, by using a stepwise gradient from 1:19, 1:9, and 1:6 (EtOAc–hexane). The appropriate fractions were pooled and evaporated, and the resulting **13** (0.404 g, 82%) was used directly in the next step. TLC 1:3 EtOAc–hexane R_f 0.52. ^{1}H NMR ($CDCl_3$) δ −0.01 (s 3 H), 0.00 (s, 3 H), 0.88 (s, 9 H), 0.89 (s, 3 H), 1.06–1.93 (m, 24 H), 1.25 (t, J = 7.2 Hz, 3 H), 2.25 (t, J = 7.4 Hz, 2 H), 3.99 (br m, 1 H), 4.12 (q, J = 7.2 Hz, 2 H). LR-MS-ES(+) m/z 566 (86, M +

dx.doi.org/10.1021/jm400032t | J. Med. Chem. XXXX, XXX, XXX–XXX

Na + CH_3CN), 525 (32, M + Na), 485 (38, M + H − H_2O), 353 (100, 485-TBSOH).

6-[(1*R*,3a*R*,4*S*,7a*R*)-4-[*tert*-Butyl(dimethyl)silyl]oxy-7a-methyl-1,2,3,3a,4,5,6,7-octahydroinden-1-yl]-1,1,1-trideuterio-10-methyl-2-(trideuteriomethyl)undecane-2,10-diol (14a). The epimeric **13** (0.404 g, 0.804 mmol) was dissolved in ether (6 mL), the solution was cooled in an ice-bath, and a 1 M solution of deuteriomethylmagnesium iodide in ether (4 mL) was added via syringe at ≤5 °C. The ice bath was then removed, and stirring continued at room temperature. TLC (1:3 EtOAc−hexane) showed a gradual conversion of the ester (R_f 0.56) to the diol **14a**, which was complete after 3 h. The solution was cooled in an ice bath, and a satd ammonium chloride solution (10 mL) was added dropwise, followed by water (5 mL) to dissolve the white precipitate. The resulting aqueous layer was re-extracted with EtOAc (30 mL), and the combined organic layers were washed with brine (10 mL containing 3 drops of 1 M HCl) then with brine (8 mL), dried, and evaporated to a colorless oil (0.4 g), which was flash-chromatographed using a stepwise gradient of 1:9, 1:6, 1:4, 1:3, and 1:2 EtOAc−hexane. Fractions were pooled and evaporated then redissolved in pentane, filtered, and evaporated to afford **14a** as a colorless, amorphous powder (0.31 g, 78%). TLC 1:3 EtOAc−hexane R_f 0.16, 1:1 EtOAc−hexane R_f 0.64. ^{1}H NMR ($CDCl_3$) δ −0.01 (s, 3H), 0.00 (s, 3H), 0.88 (s, 9H), 0.90 (s, 3H), 1.06−1.93 (m, 27H), 3.99 (br m, 1H). LR-MS-ES(+) m/z 989 (64, 2M + 1), 536 (18, M + CH_3CN + H), 495 (31, M + H), 477 (33, 495-H_2O), 459 (50, 477-H_2O), 327 (100, 459-TBSOH).

6-[(1*R*,3a*R*,4*S*,7a*R*)-4-Hydroxy-7a-methyl-1,2,3,3a,4,5,6,7-octahydroinden-1-yl]-1,1,1,11,11,11-haxadeuterio-2,10-bis-(trideuteriomethyl)undecane-2,10-diol (14b). Diol **14a** (0.31 g, 0.626 mmol) was dissolved in acetonitrile (10 mL), and a hydrofluorosilicic acid solution (35%) was added. The mixture was stirred, and the deprotection progress was monitored by TLC. After 3 h, the reaction was ca. 30% complete, another 1.5 mL of hydrofluorosilicic acid solution was added, and the mixture was stirred for a total of 24 h, at which time the reaction was complete. The mixture was equilibrated with EtOAc (60 mL) and water (20 mL), the resulting aqueous phase was re-extracted with EtOAc (20 mL), and the combined organic layers were washed with water (5 mL), dried, and concentrated. The residue was diluted with toluene and concentrated to remove acetonitrile then chromatographed on silica gel using 1:3, 1:2, and 1:1 EtOAc−hexane as mobile phases. The appropriate fractions were pooled and evaporated to furnish the triol **14b** a white, solid foam, 0.21 g, 88%. TLC 1:1 EtOAc−hexane R_f 0.34, 1:19 MeOH−DCM, R_f 0.55. ^{1}H NMR ($CDCl_3$) δ 0.91 (s, 3H), 1.09−1.63 (m, 23H), 1.70−1.88 (m, 4H), 1.92 (2H, br d), 4.05 (1H, br s). ^{13}C NMR ($CDCl_3$) δ 13.7, 17.6, 19.8, 20.0, 22.5, 26.8, 31.1, 31.2, 33.6, 38.6, 40.1, 41.9, 44.3, 44.4, 52.6, 53.0, 69.3, 70.7. LR-MS-ES(+) m/z 444 (80, M + Na + CH_3CN), 403 (48, M + Na), 363 (15, M + H − H_2O).

(1*R*,3a*R*,7a*R*)-7a-Methyl-1-[6,6,6-trideuterio-5-(trideuteriomethyl)-1-[5,5,5-trideuterio-4-(trideuteriomethyl)-4-trimethylsilyloxy-pentyl]-5-trimethylsilyloxy-hexyl]-2,3,3a,5,6,7-hexahydro-1*H*-inden-4-one (15b). Celite (0.5 g) and pyridinium dichromate (1.13 g, 3 mmol) was added to a stirred solution of triol **14b** (0.189 g, 0.496 mmol) in DCM (10 mL). The oxidation progress was followed by TLC. The reaction mixture was poured onto a column of silica gel G60 after 8 h, the column was rinsed with 1:4 EtOAc−ether (300 mL), and the residue, obtained after evaporation of solvents, was taken up in DCM and evaporated again to yield **15a** as a sticky mass. LR-MS-ES(+) m/z 442 (45, M + Na + CH_3CN), 402 (51, M + H + Na), 401 (25, M + Na), 384 (343 + CH_3CN), 361 (10, M + H − H_2O), 343 (95, M + H − H_2O-CD_3), 325 (58, 343 − H_2O). This material was directly taken up in cyclohexane (3 mL), and trimethylsilyl imidazole (0.3 mL, 2 mmol) was added. The mixture was stirred for a period of 6.5 h employing TLC 1:19 and 1:39 MeOH−DCM as process control, then diluted with hexane (10 mL) and chromatographed on a silica gel column in hexane using a stepwise gradient of hexane, 1:39, 1:19, and 1:9 EtOAc−hexane. The peak fractions were pooled and evaporated to afford the protected ketone **15b** as an oily substance (0.22 g, 85% from triol **14b**). TLC 1:19 MeOH−DCM, R_f 0.43. ^{1}H NMR ($CDCl_3$) δ 0.10 (s, 9 H), 0.11 (s, 9 H), 0.64 (s, 3 H), 1.10−2.11 (m, 22 H), 2.16−2.34 (m, 2 H), 2.46 (dd, J = 7.4 and 11.4 Hz, 1H). LR-MS-ES(+) m/z 546 (18, M + Na), 343 (100, M − 2TMSOH).

1α,25-Dihydroxy-21-(3-hydroxy-3-trideuteriomethyl-4,4,4-trideuteriobut-1-yl)-26,27-hexadeuterio-19-nor-cholecalciferol (6). A magnetically stirred 2-neck round-bottom flask equipped with thermometer and Claisen adapter containing a nitrogen sweep and rubber septum was charged with diphenylphosphine oxide **30b** (0.4209 g, 0.737 mmol) previously dried under high vacuum for 2 h. To this material was added THF (3.5 mL). The solution was stirred and cooled to −70 °C, and butyl lithium in hexane (1.6 M, 0.46 mL, 0.736 mmol) was added dropwise within 10 min. The deep cherry-red solution was stirred at −70 °C for 5 min, and then a solution of the ketone **15b** (0.2267 g, 0.433 mmol), dissolved in THF (2.5 mL), was added dropwise below −65 °C. The flask containing the ketone was rinsed with THF (1 mL), which was also added to the reactor. In process control (TLC, EtOAc−hexane 1:39 and 1:19) revealed only traces of starting material after 3 h. After an additional 45 min, the mixture was allowed to warm to −30 °C and pH 7 phosphate buffer (5 mL) was added dropwise. The mixture was stirred vigorously for 25 min. At that time, all ice had melted and the solution was transferred to a separatory funnel with the aid of hexane (40 mL). The aqueous phase was re-extracted with hexane (20 mL), and the combined hexane layers were washed with brine (5 mL), dried, and evaporated to give crude **27** as a colorless oil. This material was purified by flash chromatography using hexane and 1:79 EtOAc−hexane as mobile phases. Fractions were pooled according to TLC and evaporated to give the tetrasilyl ether **27** as a colorless oil, 0.34 g. Continued elution with EtOAc recovered the unreacted diphenylphosphine oxide **30b**. The tetrasilyl ether **27** was dissolved in a 1 M solution of tetrabutylammonium fluoride in THF (5 mL) and kept at ambient temperature for 3 h and then in the refrigerator for 48 h. The solution was then diluted with brine (10 mL), stirred for 10 min, and water (20 mL) was added to dissolve precipitated salt. This mixture was equilibrated with EtOAc (40 mL), and the aqueous phase was re-extracted with EtOAc (20 mL); the combined extracts were washed with water (5 × 10 mL) and then with brine (5 mL), dried, and evaporated to a colorless oil that was taken up in 2:1 EtOAc−hexane and charged to a flash column, using stepwise gradients of 2:1 and 4:1 EtOAc−hexane, EtOAc, and 1:9 MeOH−EtOAc as mobile phases. Fractions containing a minor quantity of partially desilylated material preceded the product band. These fractions were pooled and evaporated to give the tetraol **6** as white solid residue. This material was dissolved in methyl formate to which a few drops of MeOH were added to achieve complete dissolution. The resulting solution was filtered and concentrated, then flash evaporated and dried under high vacuum for 3 h to furnish **6** as an amorphous powder (183 mg, 84% from **15b**); $[\alpha]_D$ +51.0 (MeOH, c 0.253). ^{1}H NMR (400 MHz, CD_3Cl) δ 0.53 (s, 3 H), 1.14−2.08 (m, 30 H), 2.14−2.26 (m, 2 H), 2.47 (d, J = 10.9 Hz, 1 H), 2.68−2.85 (m, 2 H), 3.96−4.16 (m, 2H), 5.85 (d, J = 11.1 Hz, 1 H), 6.30 (d, J = 11.3 Hz, 1 H) ppm. ^{13}C NMR 12.2, 19.8, 20.1, 22.18, 23.5, 27.1, 29.0, 31.3, 37.2, 39.4, 40.2, 42.2, 44.3, 44.4, 44.6, 45.8, 53.0, 56.3, 67.1, 67.3, 70.8, 115.2, 123.6, 131.2, 142.8 ppm. UV_{max} (ε) 243 (32529), 251 (37925), 261 (25718) nm. LR-ES(+) m/z 566 (55, M + Na + CH_3CN), 525 (29, M + Na), 503 (13, M + H), 467 (55, 503-2H_2O), 449 (16, 467-H_2O), 431 (449-H_2O). HR-ES(+) calcd for M + Na 531.4291, found 531.4289.

Ethyl (5*S*)-5-[(1*R*,3a*R*,4*S*,7a*R*)-4-[*tert*-Butyl(dimethyl)silyl]-oxy-7a-methyl-1,2,3,3a,4,5,6,7-octahydroinden-1-yl]-9-hydroxy-9-methyl-decanoate (19). A mixture of zinc powder (0.600 g, 9.18 mmol), pyridine (11.2 mL), and ethyl acrylate (1.0 mL, 0.918 g, 9.17 mmol) was stirred vigorously, and nickel chloride hexahydrate (0.5364 g, 2.26 mmol) was added. The gray suspension was processed as described for **13**, and then a solution of the iodo compound **18** (1.02 g, 1.95 mmol) in pyridine (7 mL) was added dropwise over a period of 20 min, followed by pyridine rinses (2 × 2 mL). The ice bath was removed, and stirring continued at ambient temperature for 2 h. At that time, **18** was no longer detectable (TLC 1:3 EtOAc−hexane, R_f

0.70). The mixture was then poured into EtOAc (50 mL), the mixture was filtered through Celite, filter cake was washed with EtOAc (40 mL), and the combined filtrate and washings were sequentially equilibrated with 1 M HCl (50 mL), 0.5 M HCl (50 mL), and 2 M phosphoric acid (40 mL). The solution was then washed with brine (2 × 15 mL), dried ($MgSO_4$), and evaporated. The resulting residue (1.15 g) was flash chromatographed using 1:19, 1:9, and 1:6 EtOAc−hexane as mobile phases. The homogeneous fractions were pooled and evaporated. The residue was evaporated twice from hexane then dried to give **19** (0.82 g, 85%). TLC (1:3 EtOAc−hexane) R_f 0.52; $[\alpha]_D$ +31.5 (chloroform, *c* 0.308). IR ($CHCl_3$) ν C═O (1724 cm^{-1}). ^1H NMR ($CDCl_3$) δ −0.01 (s, 3 H), 0.00 (s, 3 H), 0.88 (s 9 H), 0.89 (s 3 H), 1.06−1.93 (m, 24 H), 1.21 (s, 6H), 1.25 (t, *J* = 7.2 Hz, 3 H), 2.25 (t, *J* = 7.4 Hz, 2H), 3.98 (br m, 1 H), 4.12 (q, *J* = 7.2 Hz). ^{13}C NMR ($CDCl_3$) δ −5.0, −4.7, 14.0, 14.4, 17.8, 18.1, 20.0, 20.9, 23.0, 25.9, 26.8, 29.3, 29.4, 30.1, 31.2, 34.5, 34.8, 38.4, 40.4, 42.2, 44.5, 53,0, 53.1, 60.2, 69.4, 71.0, 173.8. LR-ES(+) *m/z* 560 (14, M + Na + CH_3CN), 519 (10, M + Na), 479 (19, M + H − H_2O), 347 (100, 479-TBSOH).

(6*S*)-6-[(1*R*,3a*R*,4*S*,7a*R*)-4-[*tert*-Butyl(dimethyl)silyl]oxy-7a-methyl-1,2,3,3a,4,5,6,7-octahydroinden-1-yl]-1,1,1-trideuterio-10-methyl-2-(trideuteriomethyl)undecane-2,10-diol (20a). A solution of monoester **19** (0.69 g, 1.39 mmol) in ether (10 mL) was treated with a 1 M solution of deuteriomethylmagnesium iodide in ether (6.8 mL) and worked up as described for **14a** to afford **20a** as a colorless oil (0.94 g), which was chromatographed on a flash column using 1:9, 1:6, 1:4, 1:3, and 1:2 EtOAc−hexane as stepwise gradients. Fractions were pooled and evaporated to leave a residue that was taken up in pentane and then filtered and evaporated to give **20a** as a colorless amorphous solid (0.57 g, 84%). TLC (1:3 EtOAc−hexane) R_f 0.11. ^1H NMR ($CDCl_3$) δ −0.01 (s, 3 H), 0.00 (s, 3 H), 0.88 (s, 9 H), 0.90 (s 3 H), 1.07−1.84 (m, 26 H), 1.21 (s 6 H), 1.89 (m, 1 H), 3.99 (br m, 1 H). LR-ES(+) *m/z* 511 (4, M + Na), 471 (10, M + H − H_2O), 453 (28, 471-H_2O), 357 (5, M + H − TBSOH), 339 (12, 471-TBSOH), 321 (100, 453-TBSOH).

(6*S*)-6-[(1*R*,3a*R*,4*S*,7a*R*)-4-Hydroxy-7a-methyl-1,2,3,3a,4,5,6,7-octahydroinden-1-yl]-1,1,1-trideuterio-10-methyl-2-(trideuteriomethyl)undecane-2,10-diol (20b). A solution of **20a** (0.54 g, 0.110 mmol) in acetonitrile (20 mL) was stirred, and a 35% hydrofluorosilicic acid solution (3 mL) was added. The hydrolysis was complete after 15 h, as evidenced by the disappearance of **20a** (TLC 1:1 EtOAc−hexane, R_f 0.64). The solution was equilibrated with EtOAc (60 mL) and water (20 mL), the aqueous layer was extracted with EtOAc (25 mL), and the combined organic layers were washed with water (8 mL). The resulting organic layer was dried and concentrated, and the residue was diluted with toluene and concentrated to remove acetonitrile and then chromatographed using 1:3, 1:2, and 1:1 EtOAc−hexane as mobile phases. Pooled fractions were evaporated, and the residue was coevaporated twice from hexane, taken up in 1:1 DCM−hexane, filtered, and evaporated again and dried to leave the triol **20b** as an amorphous powder (0.36 g, 87%). TLC (1:1 EtOAc−hexane) R_f 0.34; $[\alpha]_D$ +25.2 (MeOH, *c* 0.306). ^1H NMR ($CDCl_3$) δ 0.92 (s, 3 H), 1.10−1.66 (m, 24H), 1.21 (s, 6 H), 1.67−1.90 (m, 3 H), 1.94 (br m, 1H), 4.07 (br m, 1 H). ^{13}C NMR ($CDCl_3$) δ 13.7, 17.6, 19.8, 20.1, 22.5, 26.8, 29.3, 29.4, 31.1, 31.3, 33.7, 38.7, 40.1, 44.3, 44.6, 52.6, 53.0, 69.4, 71.05. LR-MS-ES(+) *m/z* 438 (18, M + Na + CH_3CN), 397 (34, M + Na), 357 (20, M + H − H_2O), 339 (54, 357-H_2O), 321 (100, 339-H_2O).

(1*R*,3a*R*,7a*R*)-7a-Methyl-1-[(1*S*)-6,6,6-trideuterio-5-hydroxy-1-(4-hydroxy-4-methyl-pentyl)-5-(trideuteriomethyl)hexyl]-2,3,3a,5,6,7-hexahydro-1*H*-inden-4-one (21a). A solution of **20b** (0.35 g, 0.934 mmol) in DCM (20 mL) was stirred vigorously, and Celite (1 g) was added followed by pyridinium dichromate (2.26 g, 6 mmol). The oxidation was complete after 4 h. The reaction mixture was poured onto a column of silica gel G60, and the column was rinsed with 1:4 EtOAc−ether (300 mL). The residue obtained after evaporation of the column effluent was taken up in DCM, evaporated to a foam, and dried to afford the ketone **21a** (0.32 g, 92%). TLC (1:19 MeOH−DCM) R_f 0.32. IR ($CHCl_3$) ν C═O (1705 cm^{-1}), LR-ES(+) *m/z* 396 (20, 355 + CH_3CN), 378 (337 + CH_3CN), 355 (8, M + H − H_2O), 337 (50, 355-H_2O), 319 (48, 337-H_2O).

(1*R*,3a*R*,7a*R*)-7a-Methyl-1-[(1*S*)-6,6,6-trideuterio-1-(4-methyl-4-trimethylsilyloxy-pentyl)-5-(trideuteriomethyl)-5-trimethylsilyloxy-hexyl]-2,3,3a,5,6,7-hexahydro-1*H*-inden-4-one (21b). Trimethylsilyl imidazole (0.6 mL, 4 mmol) was added to the suspension of **21a** (0.32 g, 0.859 mmol) in cyclohexane (6 mL). The starting material dissolved, and a new suspension formed within minutes which was stirred overnight, diluted with hexane (10 mL), and charged to a silica gel column. Elution with 1:39 and 1:19 EtOAc−hexane, pooling of appropriate fractions, and evaporation gave a residue that was coevaporated from hexane and dried to give **21b** as an oily substance. TLC 1:19 MeOH−DCM (R_f 0.91) and 1:39 EtOAc−hexane (R_f 0.09). This material was divided into two nearly equal parts and used directly for the syntheses of **7a** and **7b** as described below.

1,25-Dihydroxy-21-(3-hydroxy-3-trideuteriomethyl-4,4,4-trideuteriobut-1-yl)-cholecalciferol (7a). A 25 mL 2-neck flask equipped with thermometer, Claisen adapter containing a nitrogen sweep, and rubber septum was charged with the diphenylphosphine oxide **30a** (0.5001 g, 0.858 mmol) previously dried for 3 h. This material was dissolved in THF and cooled to −70 °C, and 2 M phenyllithium in hexane (0.43 mL) was added within 10 min. The deep orange-colored solution was stirred at −70 °C for 5 min, then a solution of the ketone **21b** (0.227 g, 0.439 mmol), dissolved in THF (3 mL), was added dropwise below −65 °C during 30 min. The flask containing the ketone was rinsed with THF (1 mL), and this rinse was also added to the reactor after 2 h. The mixture was stirred for an additional 30 min. At that time, **21b** (TLC 1:39, R_f 0.10 and 1:19 EtOAc−hexane, R_f 0.37) was converted to **28a** (TLC 1:39, R_f 0.30 and 1:19 EtOAc−hexane, R_f 0.73). Thus, the mixture was allowed to warm to −30 °C, and pH 7 phosphate buffer (5 mL) was added dropwise. The mixture was stirred vigorously for 25 min. At that time, all ice had melted and the solution was equilibrated with hexane (40 mL). The aqueous phase was re-extracted with hexane (20 mL). The combined extracts were washed with brine (5 mL), dried, and evaporated to give the crude tetrasilyl ether **28a** as a colorless oil. This material was dissolved in hexane and charged onto a flash column, which was eluted with hexane and 1:79 EtOAc−hexane. Fractions were pooled and evaporated, and the residue coevaporated once from hexane to give **28a** (0.36 g) as a colorless oily residue. This material was dissolved in a 1 M solution of tetrabutylammonium fluoride in THF (6 mL) and kept at room temperature for 29 h. This mixture was then equilibrated with EtOAc (40 mL). The aqueous phase was extracted with EtOAc (20 mL), and the combined extracts were washed with water (5 × 10 mL) and then with brine (5 mL), dried, and evaporated to leave a colorless oil that was taken up in 2:1 EtOAc−hexane and charged to a flash column using 2:1, 4:1, and EtOAc as stepwise gradients. Fractions were pooled and evaporated, the residue was dissolved in methyl formate, the solution filtered and concentrated, and the residue was flash evaporated and dried for 3 h to afford **7a** as amorphous solids (0.1909 g, 85%), $[\alpha]_D$ +16.0 (*c* 0.32, MeOH). ^1H NMR ($CDCl_3$) δ 0.50 (s, 3H), 1.05 (s, 6H), 1.10−1.54 (m, 19H, 1.56−1.71 (m, 3H), 1.72−1.84 (m, 2H), 1.84−2.00 (m, 2H), 2.16 (dd, *J* = 13.5, 5.6 Hz, 1H), 2.36 (d, *J* = 11.1 Hz, 1H), 2.72−2.87 (m, 1H), 3.90−4.08 (m, 3H), 4.12−4.27 (m, 1H), 4.55 (d, *J* = 3 Hz), 1H), 4.76 (d, *J* = 2.1 Hz, 1H), 4.86 (d, *J* = 4.7 Hz, 1H), 5.22 (d, *J* = 1.3 Hz), 5.99 (d, *J* = 11.1 Hz, 1H), 6.19 (d, *J* = 11.3 Hz, 1H). ^{13}C NMR ($CDCl_3$) δ 11.9, 19.5, 19.7, 21.8, 23.2, 26.7, 28.4, 29.2, 29.4, 31.1, 31.2, 38.7, 38.9, 39.0, 39.1, 39.3, 39.5, 39.6, 39.7, 39.9, 40.1, 43.1, 44.1, 44.3, 44.9, 45.3, 50.5, 52.5, 55.6, 65.0, 68.4, 68.5, 68.7, 109.9, 117.4, 122.4, 135.7, 140.0, 149.3. UV_{max} (ε) 211 (14747), 265 (15897). HR-ES(+) calcd for $C_{32}H_{48}D_6O_4$ + Na 531.4291, found 531.4290.

1,25-Dihydroxy-21-(3-hydroxy-3-trideuteriomethyl-4,4,4-trideuteriobut-1-yl)-19-nor-cholecalciferol (7b). The protocol described above was repeated using diphenylphosphine oxide **30b** (0.4289 g, 0.755 mmol), 1.6 M butyl lithium in hexane (0.47 mL 0.755 mmol), and **21b** (0.2055 g, 0.397 mmol). The resulting **28b** was taken up in a 1 M solution of tetrabutylammonium fluoride in THF (5 mL), and the solution was kept at room temperature for 47 h. Following an extractive isolation as described above, **21a** was obtained as a colorless oil that was taken up in 2:1 EtOAc−hexane and charged to a flash column which was eluted with 1:9, 2:1, 4:1 EtOAc−hexane, EtOAc,

dx.doi.org/10.1021/jm400032t | J. Med. Chem. XXXX, XXX, XXX−XXX

and MeOAc. Fractions were pooled and evaporated. The white residue obtained was evaporated twice with hexane and the resulting residue (0.1 g) dissolved in methyl formate to which a few drops of MeOH were added to ensure complete dissolution. This solution was filtered and concentrated then evaporated and dried to give **7b** as an amorphous solid (0.118 g, 60%); $[\alpha]_D$ +53.8 (*c* 0.31, MeOH). ^{1}H NMR δ 0.50 (s, 3H), 1.06 (s, 6H), 1.13−1.73 (m, 23H), 1.71−2.10 (m, 5H), 2.26 (d, *J* = 10.7 Hz, 1H), 2.38−2.46 (m, 1H), 2.62−2.86 (m, 1H), 3.75−3.91 (m, 2H), 3.94−4.18 (m, 2H), 4.23−4.69 (m, 2H), 5.79 (d, *J* = 11.1 Hz), 6.07 (s, *J* = 11.1 Hz). ^{13}C NMR δ 12.1, 19.5, 19.8, 21.8, 23.1, 26.8, 28.3, 29.2, 29.4, 31.1, 31.2, 37.0, 38.9, 39.1, 39.3, 39.5, 39.7, 39.9, 40.1, 42.2, 44.1, 44.4, 44.6, 45.2, 52.6, 55.6, 65.3, 65.6, 68.5, 68.8, 115.9, 120.9, 134.5, 139.4. UV_{max} (ε) 243 (31661), 252 (36406), 261 (24892). LR-ES(+) *m/z* 461 (50, M + H − H_2O), 443 (28, 461-H_2O), 275 (100, M − $C_{13}H_{22}D_6O_2$ + H). HR-ES(+) calcd for $(C_{31}H_{48}D_6O_4 + Na]^+$ 519.4291, found 519.4294.

Ethyl (5*R*)-5-[(1*R*,3a*R*,4*S*,7a*R*)-4-[*tert*-Butyl(dimethyl)silyl]-oxy-7a-methyl-1,2,3,3a,4,5,6,7-octahydroinden-1-yl]-9-hydroxy-9-methyl-decanoate (24). Zn powder (1.12 g, 17.13 mmol), pyridine (I20 g), ethyl acrylate (1.87 mL, 17.13 mmol, 1.715 g), nickel chloride hexahydrate (1.00 g, 4.22 mmol), and iodide **23** (1.91 g, 3.65 mmol) in pyridine (13 mL) was processed as described for **13** TLC (1:3 ethyl acetate−hexane) to achieve a complete conversion of **23** (R_f 0.57) to the ester **24** (R_f 0.52). The mixture was then poured into EtOAc (80 mL), the resulting suspension was filtered through Celite, and the filter cake was washed with EtOAc (40 mL). Filtrate and washings were combined and equilibrated with 2 M phosphoric acid, and the slightly acidic extract was washed with brine (5 mL), dried, and evaporated. The residue was flash chromatographed using hexane and 1:19 and 1:9 EtOAc−hexane as stepwise gradient. Homogeneous fractions were pooled and evaporated (0.64 g), tale fractions were also pooled and evaporated and purifies by preparative HPLC on a 2 in. × 18 in. 15−20 μ silica YMC HPLC column using 1:3 EtOAc−hexane as mobile phase and running at 100 mL/min to afford additional pure **24** (peak volume: 1.85 L, 1.01 g of residue), total yield 1.65 g, 86%. TLC 1:2 EtOAc−hexane, R_f 0.70; $[\alpha]_D$ +12.2 (chloroform, *c* 0.262). IR ($CHCl_3$) ν C=O (1725 cm^{-1}). ^{1}H NMR ($CDCl_3$) δ −0.01 (s, 3 H), 0.0 (s 3 H), 0.88 (s, 9 H), 0.89 (s, 3 H), 1.06−1.93 (m, 24 H), 1.21 (s, 6 H), 1.25 (t, *J* = 7.2 Hz, 3 H), 2.26 (m, 2 H), 3.98 (br m, 1 H), 4.12 (q, *J* = 7.2 Hz, 2H). ^{13}C NMR ($CDCl_3$) δ 13.9, 14.4, 17.8, 19.9, 21.0, 23.0, 25.9, 26.8, 29.3, 29.4, 30.2, 31.1, 34.5, 34.9, 38.5, 40.5, 42.2, 44.4, 53.0, 53.1, 60.2, 69.4, 71.0, 76.5, 173.8. LR-ES(+) *m/z* 993 (32 2M + 1), 560 (18, M + Na + CH_3CN), 479 (54, M + H − H_2O), 347 (72, M − H_2O − THSOH).

(6*R*)-6-[(1*R*,3a*R*,4*S*,7a*R*)-4-[*tert*-Butyl(dimethyl)silyl]oxy-7a-methyl-1,2,3,3a,4,5,6,7-octahydroinden-1-yl]-1,1,1-trideuterio-10-methyl-2-(trideuteriomethyl)undecane-2,10-diol (25a). A solution of the ester **24** (1.50 g, 3.02 mmol) in ether (20 mL) was treated with a 1 M solution of deuteriomethylmagnesium iodide in ether (16 mL) as described previously. The resulting oily **25a** (1.63 g) was chromatographed as described to afford a residue (1.43 g) which was taken up in pentane, filtered, concentrated, flash evaporated, and dried to yield **25a** as a colorless powder (1.32 g, 89%). TLC 1:2 EtOAc−hexane, R_f 0.37. LR-ES(+) *m/z* 453 (35, M + H − $2H_2O$). ^{1}H NMR ($CDCl_3$) δ −0.01 (s, 3 H), 0.00 (s, 3 H), 0.88 (s, 9 H), 0.90 (s, 3 H), 1.07−1.61 (m, 23H), 1.21 (s, 6 H), 1.62−1.85 (m, 3 H), 1.89 (br m, 1 H), 3.99 (br m, 1 H).

(6*R*)-6-[(1*R*,3a*R*,4*S*,7a*R*)-4-Hydroxy-7a-methyl-1,2,3,3a,4,5,6,7-octahydroinden-1-yl]-1,1,1-trideuterio-10-methyl-2-(trideuteriomethyl)undecane-2,10-diol (25b). A solution of the tetrasilyl ether **25a** (1.32 g, 0.110 mmol) in a mixture of THF (5 mL) and acetonitrile (45 mL) was further diluted with a hydrofluorosilicic acid solution (35%, 7.5 mL). The conversion of **25a** (TLC 1:1 EtOAc−hexane, R_f 0.64) to **25b** (R_f 0.34) was complete after 14.5 h. The solution was diluted with EtOAc (120 mL) and water (40 mL) and processed as described for **20b** to afford **25b** as an amorphous powder, 0.87 g (86%). TLC 1:19 MeOH−DCM R_f 0.30; $[\alpha]_D$ +23.9 (MeOH), *c* 0.426). ^{1}H NMR ($CDCl_3$) δ 0.93 (s, 3H), 1.12−1.55 (m, 28H), 1.73−1.86 (3H, m), 1.90−1.98 (1H, m), 4.07 (1H, m) ppm. ^{13}C NMR ($CDCl_3$) δ 13.7, 17.6, 19.9, 20.1, 22.5, 26.8, 29.3, 29.4, 31.1, 31.3, 33.7, 38.7, 40.1, 42.0, 44.4, 52.6, 53.0, 69.4, 70.8, 71.0. *m/z* 497 (22, M + CH_3CN − H_2O), 369 (20, M + Na − H), 357 (39, M + H − H_2O), 339 (58, 357 − H_2O). LR-ES(+) *m/z* 397 (15, M + Na), 357 (33, M + H − H_2O), 339 (357-H_2O). LR-ES(−) *m/z* 409 (80, M + Cl).

(1*R*,3a*R*,7a*R*)-7a-Methyl-1-[(1*R*)-6,6,6-trideuterio-5-hydroxy-1-(4-hydroxy-4-methyl-pentyl)-5-(trideuteriomethyl)hexyl]-2,3,3a,5,6,7-hexahydro-1*H*-inden-4-one (26a). A mixture of the triol **25b** (0.45 g. 1.20 mmol), DCM (25 mL), and Celite (1.2 g) was treated with pyridinium dichromate (2.71 g, 7.3 mmol) as described for **21a** to yield ketone **26a** (0.44 g, 98%) as an amorphous powder, TLC 1:19 MeOH−DCM 0.36, IR ($CHCl_3$) ν C=O (1705 cm^{-1}), LR-ES(+) *m/z* 396 (40, M + H + CH_3CN − H_2O), 378 (24, 337 + CH_3CN), 355 (8, M + H − H_2O), 337 (100, 355-H_2O), 319 (59, 337-H_2O).

(1*R*,3a*R*,7a*R*)-7a-Methyl-1-[(1*R*)-6,6,6-trideuterio-1-(4-methyl-4-trimethylsilyloxy-pentyl)-5-(trideuteriomethyl)-5-trimethylsilyloxy-hexyl]-2,3,3a,5,6,7-hexahydro-1*H*-inden-4-one (26b). Trimethylsilyl imidazole (0.75 mL, 4 mmol) was added to a suspension of **26a** (0.44 g, 1.18 mmol) in cyclohexane (8 mL) and processed as described for **21b** to furnish the disilyl ether **26b** (0.59 g, 96%) as a colorless syrup. TLC 1:19 MeOH−DCM, R_f 0.91, and 1:19 EtOAc−hexane, R_f 0.30. ^{1}H NMR ($CDCl_3$) δ 0.10 (s, 9 H), 0.11 (s, 9 H), 0.64 (s, 3 H), 1.10−2.11 (m, 22 H), 1.21 (s, 6 H), 2.16−2.34 (m, 2 H), 2.46 (dd, *J* = 7.4 and 11.4 Hz, 1 H). This material was split into two nearly equal parts and used for the synthesis of **8a** and **8b**.

[(1*S*,3*Z*,5*R*)-3-[(2*E*)-2-[(1*R*,3a*S*,7a*R*)-7a-Methyl-1-[(1*R*)-6,6,6-trideuterio-1-(4-methyl-4-trimethylsilyloxy-pentyl)-5-(trideuteriomethyl)-5-trimethylsilyloxy-hexyl]-2,3,3a,5,6,7-hexahydro-1*H*-inden-4-ylidene]ethylidene]-5-[*tert*-butyl(dimethyl)-silyl]oxy-2-methylene-cyclohexoxy]-*tert*-butyl-dimethyl-silane (29a). Diphenylphosphine oxide **30a** (0.5238 g, 0.899 mmol) was deprotonated and coupled to the ketone **26b** (0.2942 g, 0.569 mmol) as described for **28a** to yield crude **29a**. This material was dissolved in hexane and flash-chromatographed using a stepwise gradient of hexane and 1:79 EtOAc−hexane to remove some unreacted ketone (TLC, 1:19 EtOAc−hexane, R_f 0.33). Homogeneous fractions were pooled and evaporated. The colorless residue was coevaporated once from hexane, to give **29a** (0.30 g, 60%) as a colorless oily residue. TLC (1:19 EtOAc−hexane) R_f 0.73, (1:39 EtOAc−hexane) R_f 0.27. LR-ES(+) *m/z* 881 (15, M + H), 659 (12, M + H − TMSOH − TBSOH).

1α,25-Dihydroxy-21-(3-hydroxy-3-methyl-but-1-yl)-26,27-hexadeuterio-cholecalciferol (8a). The residue obtained above was dissolved in a 1 M solution of tetrabutylammonium fluoride in THF (6 mL) and kept at room temperature for 30 h. The solution was diluted with brine (10 mL) and stirred for 10 min, and then water (5 mL) was added to dissolve precipitated salt. This mixture was equilibrated with EtOAc (40 mL) and then worked up and purified as described for **7a** to yield **8a** as amorphous solids (0.151 g, 87%). TLC (EtOAc) R_f 0.64; $[\alpha]_D$ +11.9° (MeOH, *c* 0.16). UV_{max} (MeOH) ε 211 (16548), 266 nm (16932). ^{1}H NMR (DMSO-d_6) δ 0.50 (s, 3H), 1.06 (s, 9H), 1.10−1.53 (m, 19H), 1.57−1.69 (m, 3H), 1.71−1.84 (m, 2H), 1.89 (d, *J* = 10.7 Hz, 1H), 1.93−2.02 (m, 1H), 2.16 (dd, *J* = 14.0, 6.1 Hz), 2.36 (d, 11.1 Hz, 1H), 2.79 (d, *J* = 8.7 Hz, 1H), 3.99 (br s, 1H), 4.01 (s, 1H), 4.04 (s, 1H), 4.19 (br s, 1H), 4.54 (d, *J* = 3.6 Hz, 1H), 4.85 (d, *J* = 4.9 Hz, 1H), 5.22 (br s, 1H), 5.99 (d *J* = 11.5 Hz, 1H), 6.19 (d, *J* = 11.7 Hz). ^{13}C NMR (DMSO-d_6) 11.9, 19.5, 19.7, 21.8, 23.2, 26.7, 28.4, 29.2, 29.4, 31.1, 31.2, 38.7, 38.9, 39.1, 39.3, 39.5, 39.7, 39.9, 40.1, 43.1, 44.2, 44.9, 45.3, 52.5, 55.6, 65.0, 68.4, 68.5, 68.2, 109.9, 117.4, 122.4, 135.7, 140.0, 149.3. LR-ES(+) *m/z* 509 (15, M + H), 491 (34, M + H − H_2O), 473 (100, 491-H_2O), 455 (60, 473-H_2O), 437 (15, 455-H_2O).

[(1*R*,5*R*)-3-[(2*E*)-2-[(1*R*,3a*S*,7a*R*)-7a-Methyl-1-[(1*R*)-6,6,6-trideuterio-1-(4-methyl-4-trimethylsilyloxy-pentyl)-5-(trideuteriomethyl)-5-trimethylsilyloxy-hexyl]-2,3,3a,5,6,7-hexahydro-1*H*-inden-4-ylidene]ethylidene]-5-[tert-butyl(dimethyl)silyl]-oxy-cyclohexoxy]-*tert*-butyl-dimethyl-silane (29b). The protocol for **7b** was repeated using diphenylphosphine oxide **30b** (0.5844 g, 1.02 mmol, 1.82 equiv) and ketone **26b** (0.2833 g, 0.548 mmol) to furnish **29b** (0.41 g, 77%) as a colorless oil. TLC (1:19 EtOAc−

dx.doi.org/10.1021/jm400032t | *J. Med. Chem.* XXXX, XXX, XXX−XXX

hexane) R_f 0.75. ^{1}H NMR ($CDCl_3$) δ 0.4 (s, 3H), 0.05 (s, 6H), 0.06 (s, 3H), 0.10 (s, 18H), 0.53 (s, 3H), 0.86 (s, 9H), 0.87 (s, 9H), 1.11−1.73 (m, 21H), 1.20 (s, 6H), 1.74−1.89 (m, 3H), 1.94 (br d, $J \sim 12.1$ and 1 Hz, 1H), 2.00 (brt, $J \sim 9.6$ and 1 Hz), 2.10 (dd, $J = 7.4$ and 13.1 Hz, 1H), 2.26 (dd, $J \sim 2.7$ and 13.4 Hz, 1H), 2.34−2.42 (m, 2H), 2.81 (br m, 1H), 4.02−4.12 (m, 2H), 5.82 (d, $J = 11.2$ Hz, 1H), 6.17 (d, $J = 11.2$ Hz, 1H).

1,25-Dihydroxy-21-(3-hydroxy-3-methyl-but-1-yl)-19-nor-26,27-hexadeuterio-cholecalciferol (8b). The tetrasilyl ether **29b** obtained above (0.41 g, 0.471 mmol) was dissolved in a 1 M solution of tetrabutylammonium fluoride in THF (8 mL). The deprotection was complete after 62 h at room temperature. The solution was diluted with brine (15 mL), stirred for 10 min, and then equilibrated with the EtOAc (50 mL) and treated as described for deprotection of **28b** to afford **8b** as an amorphous powder (0.202 g, 86%). TLC (EtOAc) R_f 0.36; $[\alpha]_D$ +54.5 (MeOH, *c* 0.398). UV_{max} (ε) 243 (25005), 251 (29167), 261 (19777) nm (MeOH). ^{1}H NMR (DMSO-d_6) δ 0.50 (s, 3H), 1.05 (s, 6H), 1.10−1.72 (m, 23H), 1.73−1.85 (m, 1H), 1.90 (d, $J = 11.3$ Hz), 1.94−2.11 (m, 3H), 2.19−2.32 (m, 1H), 2.38−2.47 (m, 1H), 2.63−2.84 (m, 1H), 3.73−3.93 (m, 2H), 4.04 (d, 8.5 Hz, 2H), 4.38 (d, $J = 3.4$ Hz), 4.49 (d, $J = 3.6$ Hz), 5.80 (d, $J = 11.1$ Hz), 6.08 (d, $J = 11.1$ Hz, 1H). ^{13}C NMR δ 12.0, 19.5, 19.7, 21.7, 23.1, 26.8, 28.3, 29.2, 29.4, 31.1, 31.2, 37.00, 38.7, 38.9, 39.1, 39.3, 39.5, 39.7, 39.9, 40.1, 42.2, 44.2, 44.6, 45.2, 52.5, 55.6, 65.3, 65.5, 68.4, 68.7, 115.9, 129.9, 134.5, 139.4. LR-ES(+) *m*/*z* 497 (6, M + H − H_2O), 461 (78, 479-H_2O), 443 (20, 461-H_2O), 425 (6, 443-H_2O). HR-ES(+) calcd for $C_{31}H_{48}D_6O_4$ + Na 519.4291, found 519.4290.

■ ASSOCIATED CONTENT

Ⓢ Supporting Information

Analytical data for final compounds and crystal data, including refinement characteristics. This material is available free of charge via the Internet at http://pubs.acs.org.

Accession Codes

The PDB ID codes shown below are also included in the Supporting Information. PDB ID: 4IA2 (**7a**); 4IA1 (**7b**); 4IA3 (**8a**); 4IA7 (**8b**).

■ AUTHOR INFORMATION

Corresponding Author

*Phone: (973) 831-1591. E-mail: hubert.maehr@verizon.net.

Present Address

‖For H.J.L.: Department of Food Science and Technology, Chung-Ang University, Anseong Si, Gyeonggi-Do, 456−756 South Korea.

Notes

The authors declare no competing financial interest.

■ ACKNOWLEDGMENTS

We thank Alastair McEwen and the staff of the beamline ID-14-1 at ESRF for experimental assistance during data collection. We are also indebted to Bioxell Inc for chemical and Hoffmann-La Roche Inc, Nutley, NJ, for analytical support. Cell growth inhibition studies were supported in part by NIH R01 CA127645, NIEHS P30 ES005022, and by the Board of Trustees Fellowship for Scholarly Excellence at Rutgers University.

■ REFERENCES

(1) Foster, A. B. Deuterium isotope effects in the metabolism of drugs and xenobiotics: implications for drug design. *Adv. Drug Res.* **1985**, *1*, 2.

(2) Mutlib, A. E. Application of stable labeled compounds in metabolism and in metabolism-mediated toxicity studies. *Chem. Res. Toxicol.* **2008**, 1672−1689.

(3) Kushner, D. J.; Baker, A.; Dunstall, T. G. Pharmacological uses and perspectives of heavy water and deuterated compounds. *Can. J. Physiol. Pharmacol.* **1999**, *77*, 79−88.

(4) Carlberg, C. Molecular basis of the selective activity of vitamin D analogues. *J. Cell. Biochem.* **2003**, *88*, 274−281.

(5) Yang, W.; Freedman, L. P. 20-Epi analogues of 1,25-dihydroxyvitamin D_3 are highly potent inducers of DRIP coactivator complex binding to the vitamin D_3 receptor. *J. Biol. Chem.* **1999**, *274*, 16836−16845.

(6) Rachez, C.; Suldan, Z.; Ward, J.; Chang, C-P; Burakov, D.; Erdjument-Bromage, H.; Tempst, P.; Freedman, L. P. A novel protein complex that interacts with the vitamin D_3 receptor in a ligand-dependent manner and enhances VDR transactivation in a cell-free system. *Genes Dev.* **1998**, *12*, 1787−1800.

(7) Norman, A. W.; Manchand, P. S.; Uskokovic, M. R.; Okamura, W. H.; Takeuchi, J. A.; Bishop, J. E.; Hisatake, J-I; Koeffler, H. P.; Peleg, S. Characterization of a novel analog of 1α,25(OH)$_2$-vitamin D_3 with two side chains: interaction with its nuclear receptor and cellular action. *J. Med. Chem.* **2000**, *43*, 2719−2730.

(8) Uskokovic, M. R; Maehr, H.; Reddy, S. G; Li, Y. C.; Adorini, L.; Holick, M. F. Gemini: the 1,25-dihydroxy vitamin D analogs with two side-chains. *Vitamin D*, 2nd ed.; Feldman, D., Pike, J. W., Glorieux, F. H., Eds.; Elsevier Academic Press: London, 2005; pp 1511−1524.

(9) Lee, H. J.; Ji, Y.; Paul, S.; Maehr, H.; Uskokovic, M.; Suh, N. Activation of bone morphogenetic protein signaling by a gemini vitamin D3 analogue is mediated by Ras/protein kinase Cα. *Cancer Res.* **2007**, *67*, 11840−11847.

(10) Lee, H. J.; Paul, S.; Atalla, N.; Thomas, P. E.; Lin, X.; Yang, I.; Buckley, B.; Lu, G.; Zheng, X.; Lou, Y. R.; Conney, A. H.; Maehr, H.; Adorini, L.; Uskokovic, M.; Suh, N. Gemini vitamin D analogues inhibit estrogen receptor-positive and estrogen receptor-negative mammary tumorigenesis without hypercalcemic toxicity. *Cancer Prev. Res.* **2008**, *1960*, 1−9.

(11) So, J. Y.; Lee, H. J.; Smolarek, A. K.; Paul, S.; Wang, C.-X.; Maehr, H.; Uskokovic, M.; Zheng, X.; Conney, A.; Cai, L.; Liu, F.; Suh, N. A novel vitamin D analog represses the expression of stem cell marker CD44 in breast cancer. *Mol. Pharmacol.* **2011**, *79*, 360−367.

(12) Burch, W. M.; Lopez-Claros, M.; Uskokovic, M. R.; Drezner, M. K. 1,25-Dihydroxyvitamin D3 stimulates avian and mammalian cartilage growth in vitro. *J. Bone Mineral Res.* **1988**, *3*, 87−91.

(13) Sanderson, K. Big interest in heavy drugs. *Nature* **2009**, *458*, 269.

(14) Maehr, H.; Uskokovic, M. R.; Adorini, L.; Penna, G.; Mariani, R.; Panina, P.; Passini, N.; Bono, E.; Perego, S.; Biffi, M.; Holick, M.; Spina, C.; Suh, N. Calcitriol derivatives with two different side chains at C-20. III. An epimeric pair of the gemini family with unprecedented antiproliferative effects on tumor cells and renin mRNA expression inhibition. *J. Steroid Biochem. Mol. Biol.* **2007**, *103*, 277−281.

(15) Maehr, H.; Lee, H. J.; Perry, B.; Suh, N.; Uskokovic, M. R. Calcitriol derivatives with two different side chains at C20. V. Potent inhibitors of mammary carcinogenesis and inducers of leukemia differentiation. *J. Med. Chem.* **2009**, *52*, 5505−5519.

(16) Spina, C.; Tangpricha, V.; Min, Y.; Zhou, W.; Wolfe, M.; Maehr, H.; Uskokovic, M.; Adorini, L.; Holick, M. F. Colon cancer and ultraviolet B radiation and prevention and treatment of colon cancer in mice with vitamin D and its gemini analogs. *J. Steroid Biochem. Mol. Biol.* **2005**, *97*, 111−120.

(17) Reddy, G. S.; Tserng, K. Y. Calcitroic acid, end product of renal metabolism of 1,25-dihydroxyvitamin D_3 through C-24 oxidation pathway. *Biochemistry* **1989**, *28*, 1763−1769.

(18) Makin, G.; Lohnes, D.; Byford, V.; Ray, R.; Jones, G. Target cell metabolism of 1,25-dihydroxyvitamin D_3 to calcitroic acid. Evidence for a pathway in kidney and bone involving 24-oxidation. *Biochem. J.* **1989**, *262*, 173−180.

(19) Maehr, H.; Uskokovic, M. R.; Adorini, L.; Reddy, S. D. Calcitriol derivatives with two different side chains at C-20. II. Diastereoselective syntheses of the metabolically produced 24(*R*) hydroxygemini. *J. Med. Chem.* **2004**, *47*, 6478−6484.

(20) Yamada, S.; Nakayama, K.; Takayama, H.; Shinki, T.; Takasaki, Y.; Suda, T. Isolation, identification, and metabolism of (23*S*,25*R*)-hydroxyvitamin D_3-26,23-lactone. *J. Biol. Chem.* **1984**, *259*, 884−889.
(21) Horst, R. L.; Wovkulich, P. M.; Baggiolini, E. G.; Uskokovic, M. R.; Engstrom, G. W.; Napoli, J. L. (23*S*)-1,23,25-trihydroxyvitamin D_3: Its biological activity and role in 1α,25-dihydroxyvitamin D_3-26,23-lactone biosynthesis. *Biochemistry* **1984**, *23*, 3973−3976.
(22) Bouillon, R. O., W. H.; Norman, A. W. Structure−function relationships in the vitamin D endocrine system. *Endocr. Rev.* **1995**, *16*, 200−257.
(23) Guryev, O.; Carvalho, R. A.; Usanov, S.; Gilep, A.; Estabrook, R. W. A pathway for the metabolism of vitamin D_3: unique hydroxylated metaboles formed during catalysis with cytochrome P450scc (CYP11A1). *Proc. Natl. Acad. Sci. U. S. A.* **2003**, *100*, 13754−14759.
(24) Binderup, L.; Latini, S.; Binderup, E.; Bertting, C.; Calverley, M.; Hansen, K. 20-Epivitamin D3 analogues: a novel class of potent regulators of cell growth and immune responses. *Biochem. Pharmacol.* **1991**, *42*, 1569−1575.
(25) Dilworth, F. J.; Calverly, M. J.; Makin, H.; Jones, G. Increased biological activity of 20-epi-1,25-dihydroxyvitamin D3 is due to reduced catabolism and altered protein binding. *Biochem. Pharmacol.* **1994**, *47*, 987−993.
(26) Mäenpää, P. H.; Väisänen, S.; Jääskeläinen, T.; Ryhänen, S.; Rouvinen, J.; Duchier, C.; Mahonen, A. Vitamin D_3 analogs (MC 1288, KH 1060, EB 1089, GS 1558, and CB 1093): studies on their mechanism of action. *Steroids* **2001**, *66*, 223−225.
(27) Rochel, N.; Wurtz, J. M.; Mitschler, A.; Klaholz, B.; Moras, D. The crystal structure of the nuclear receptor for vitamin D, bound to its natural ligand. *Mol. Cell* **2000**, *5*, 173−9.
(28) Ciesielski, F.; Rochel, N.; Mitschler, A.; Kouzmenko, A.; Moras, D. Structural investigation of the ligand binding domain of the zebrafish VDR in complex with 1a25(OH2D3 and gemini: purification, crystallization and preliminary X-ray diffraction analysis. *J. Steroid Biochem. Mol. Biol.* **2004**, *89*−*90*, 55−59.
(29) Ciesielski, F.; Rochel, N.; Moras, D. Adaptability of the vitamin D nuclear receptor to the synthetic ligand gemini: Remodeling the LPB with one side chain rotation. *J. Steroid Biochem. Mol. Biol.* **2007**, *103*, 235−242.
(30) Rochel, N.; Moras, D. Ligand binding domain of vitamin D receptors. *Curr. Top. Med. Chem.* **2006**, *6*, 1229−41.
(31) Rochel, N.; Moras, D. Vitamin D Nuclear Receptor Ligand-Binding Domain Crystal Structure. In *Vitamin D*, 2nd ed.; Feldman, D., Pike, J. W, Glorieux, F. H., Eds.; Elsevier Academic Press: Burlington, MA, 2005; pp 279−289.
(32) Huet, T.; Maehr, H.; Lee, H. J.; Uskokovic, M. R.; Suh, N.; Moras, D.; Rochel, N. Structure−function study of gemini derivatives with two different side chains at C-20, Gemini-0072 and Gemini-0097. *Med. Chem. Commun.* **2011**, *2*, 424−429.
(33) Manchand, P. S.; Uskokovic M. R. Preparation of vitamin D_3 analogs with bis C-20 side chains as therapeutic agents. Patent WO9849138, 1998, 35 pp.
(34) Manchand P. S.; Uskokovic, M. R. Method of using vitamin D analogs with bis C-20 side chains for treating or preventing neoplastic diseases. U.S. Patent US 6008209, 1999, 13 pp.
(35) Maehr, H.; Uskokovic, M. R. Formal desymmetrization of the diastereotopic chains in gemini calcitriol derivatives with two different side chains at C-20. *Eur. J. Org. Chem.* **2004**, 1703−1713.
(36) Manchand, P. S.; Yiannikouros, G. P.; Belica, P. S.; Madan, P. Nickel-mediated conjugate addition. Elaboration of calcitriol from ergocalciferol. *J. Org. Chem.* **1995**, *60*, 6574−6581.
(37) Pilcher, A. S; DeShong, P. Improved protocols for the selective deprotection of trialkylsilyl ethers using fluorosilicic acid. *J. Org. Chem.* **1993**, *58*, 5130−5134.
(38) Baggiolin, E. G; Iacobelli, J. A.; Hennessy, B. M.; Batcho, A. D.; Sereno, J. F.; Uskokovic, M. R. Stereocontrolled total synthesis of 1.alpha.,25-dihydroxycholecalciferol and 1.alpha.,25-dihydroxyergocalciferol. *J. Org. Chem.* **1986**, *51*, 3098−3108.
(39) Daniewski, A. R.; Garofalo, L. M.; Hutchings, S. D.; Kabat, M. M.; Liu, W.; Okabe, M.; Radinov, R.; Yannikouros, G. P. Efficient synthesis of the A-ring phosphine oxide building block useful for 1α,25-dihydroxy vitamin D_3 and analogues. *J. Org. Chem.* **2002**, *67*, 1580−1587.
(40) Courtney, L. F.; Lange, M.; Uskokovic, M. R.; Wovkulich, P. M. Asymmetric synthesis of a key ring A synthon for 1α-hydroxy-19-nor vitamin D. *Tetrahedron Lett.* **1998**, *39*, 3363−3366.
(41) Zuh, G.-D.; Okamura, W. H. Synthesis of vitamin D (calciferol). *Chem. Rev.* **1995**, *95*, 1877−1952.
(42) Wade, D. Deuterium isotope effects on noncovalent interactions between molecules. *Chem.−Biol. Interact.* **1999**, *117*, 191−217.